

Leukocyte-Endothelium Interaction in the Sublingual Microcirculation of Coronary Artery Bypass Grafting Patients

Zühre Uz^{a, b} Güçlü Aykut^c Michael Massey^d Yasin Ince^a Bülent Ergin^{a, c}
Lucinda Shen^{a, c} Fevzi Toraman^e Thomas M. van Gulik^b Can Ince^{a, c}

^aDepartment of Translational Physiology, Amsterdam UMC, University of Amsterdam, Amsterdam, The Netherlands; ^bDepartment of Experimental Surgery and Translational Physiology, Amsterdam UMC, University of Amsterdam, Amsterdam, The Netherlands; ^cDepartment of Intensive Care, Erasmus MC, University Medical Center, Rotterdam, The Netherlands; ^dDepartment of Emergency Medicine, Beth Israel Deaconess Medical Center, Harvard Medical School, Boston, MA, USA; ^eDepartment of Anesthesiology and Reanimation, Acibadem Mehmet Ali Aydınlar University School of Medicine, Istanbul, Turkey

Keywords

Sublingual microcirculation · Leukocytes · Cardiac surgery · Incident dark-field imaging · Frame averaging

Abstract

Objective: The aim of this study was to apply an innovative methodology to incident dark-field (IDF) imaging in coronary artery bypass grafting (CABG) patients for the identification and quantification of rolling leukocytes along the sublingual microcirculatory endothelium. **Methods:** This study was a post hoc analysis of a prospective study that evaluated the perioperative course of the sublingual microcirculation in CABG patients. Video images were captured using IDF imaging following the induction of anesthesia (T_0) and cardiopulmonary bypass (CPB) (T_1) in 10 patients. Rolling leukocytes were identified and quantified using frame averaging, which is a technique that was developed for correctly identifying leukocytes. **Results:** The number of rolling leukocytes increased significantly from T_0 (7.5 [6.4–9.1] leukocytes/capillary-postcapillary venule/4 s) to T_1 (14.8 [13.2–15.5] leukocytes/capillary-postcapillary venule/4 s) ($p < 0.0001$). A significant increase in systemic leukocyte count was also de-

tected from $7.4 \pm 0.9 \times 10^9/L$ (preoperative) to $12.4 \pm 4.4 \times 10^9/L$ (postoperative) ($p < 0.01$). **Conclusion:** The ability to directly visualize leukocyte-endothelium interaction using IDF imaging facilitates the diagnosis of a systemic inflammatory response after CPB via the identification of rolling leukocytes. Integration of the frame averaging algorithm into the software of handheld vital microscopes may enable the use of microcirculatory leukocyte count as a real-time parameter at the bedside.

© 2019 The Author(s)
Published by S. Karger AG, Basel

Introduction

Cardiopulmonary bypass (CPB) has detrimental effects on the nature of the circulatory profile. Among others, systemic inflammatory response is an important adverse effect that cannot be ignored [1]. This syndrome results in the activation of the innate immune system, in which the leukocyte-endothelium interaction plays an

Z. Uz and G. Aykut contributed equally to this work.

important role. The leukocyte-endothelium interaction is initiated by adhesion molecules to which leukocytes embed themselves, thereby leading to leukocyte rolling, leukocyte adhesion on the endothelium, and transmigration into tissues [2–4].

Monitoring the leukocyte-endothelium interaction in the microcirculation at the bedside is a main objective in the evaluation of inflammatory response and in its therapeutic management. The ability to directly visualize the microcirculation at the bedside via handheld vital microscopy (HVM) has substantially increased the need to monitor the microcirculatory alterations in critically ill patients [5]. Imaging techniques such as orthogonal polarization spectral imaging (OPS) imaging and side-stream dark-field (SDF) or incident dark-field (IDF) imaging have been incorporated into HVM devices [6–8]. Via the application of HVM to the study of sublingual microcirculation, microcirculatory alterations have been identified in advance of alterations in systemic hemodynamic variables in many clinical settings that are associated with cardiovascular compromise, such as cardiac surgery and sepsis [9–13].

Although HVM devices are noninvasive and are feasible for bedside measurements, limited data are available on leukocyte counting and identifying the leukocyte-endothelium interaction in the human microcirculation in cardiac surgery. Bauer et al. [14] were the first to identify rolling leukocytes using HVM and a conventional manual methodology in sublingual recordings in cardiac surgery patients. However, applying the conventional methodology to OPS imaging, they were unable to distinguish between leukocytes and plasma gaps in the venules. The recent utilization of space-time diagram analysis for studying leukocyte kinetics in the sublingual microcirculation initially overcame this dilemma [15]. However, space-time diagram analysis requires specialized software such as the AVA (MicroVision Medical, Amsterdam, The Netherlands) [16], which requires time-consuming, off-line processing with multiple steps. Thus, the space-time diagram method is not directly applicable for routine clinical use [17].

Recently, the method of frame averaging was proposed for differentiating between plasma gaps and leukocytes. This methodology was first applied to SDF imaging [18], and the results demonstrated the necessity of performing additional stabilization steps prior to its use. However, the clinical advantages of applying this methodology to IDF imaging have not been previously evaluated. The ability to directly visualize the kinetics of leukocyte-endothelium interaction using IDF imaging, particularly in

cardiac surgery patients, may facilitate the diagnosis of systemic inflammatory response after CPB by identifying rolling leukocytes. Therefore, in the current study we aimed to apply the method of frame averaging to IDF imaging during CPB in coronary artery bypass grafting (CABG) patients to identify and quantify rolling leukocytes along the sublingual microcirculatory endothelium.

Methods

This study was a post hoc secondary analysis of a prospective observational study on the perioperative course of sublingual microcirculatory alterations in patients undergoing CABG. The data were obtained from 10 patients who received cold blood cardioplegia. This trial was conducted at Acibadem Mehmet Ali Aydınlar University School of Medicine, Istanbul, Turkey.

Study Population

Eligible patients were adults who were undergoing on-pump CABG surgery. The exclusion criteria were withdrawal of consent, previous heart or oral surgery, emergency surgery, ejection fraction <30%, pregnancy, history of myocardial infarction, systemic inflammatory disease, a history of immunosuppressive drugs or steroids, age <18 years, and vasculitis.

Clinical Practice

All surgeries were performed under general anesthesia. Anesthesia was induced using fentanyl (15–25 µg/kg), vecuronium (0.5 mg/kg), and propofol (1 mg/kg) and maintained via continuous propofol infusion (200–400 mg/h). The ventilation parameters were as follows: 6–8 mL/kg tidal volume, 5% end-tidal CO₂, 45% inspiratory O₂, and a positive end-expiratory pressure of 5 cm H₂O. After anesthesia induction, all patients received cefazolin 1 g as antibiotic prophylaxis and 2 g tranexamic acid as antifibrinolytic therapy. CPB was initiated after heparin administration when the activated clotting time exceeded 480 s. CPB was performed with a standard roller pump using an S3 heart-lung machine (Stöckert Sorin Group Deutschland GmbH, Munich, Germany) combined with a heater-cooler device (3M Sarns TCM II, Michigan, USA). The priming solution for CPB consisted of 1,100 mL Ringer lactate solution, 150 mL mannitol (20%), 60 mL sodium bicarbonate (8.4%), and 10,000 IU heparin. During CPB, moderate hypothermia (32–35 °C) was used. Mean arterial pressure and nonpulsatile flow rate were maintained at 40–80 mm Hg and at 2–2.5 L/min/m², respectively. Myocardial viability was preserved via topical hypothermia and antegrade cold blood cardioplegia including 120 mL ACDA, 20 mL potassium chloride (7.5%), 10 mL sodium bicarbonate (8.4%), 10 mL magnesium sulfate (15%), and 80 mL dextrose (5%). Rewarming was initiated during left internal mammary artery grafting. When body temperature reached 37 °C and the patient was hemodynamically stable, CPB was discontinued and heparin was reversed with protamine sulfate.

Microcirculatory Measurements

Microcirculatory measurements were performed sublingually with a handheld IDF camera (CytoCam, Braedius Medical, Hui-zen, The Netherlands). IDF imaging has been described extensive-

ly elsewhere [6]. Briefly, the IDF imaging technique uses green light that is produced from a ring of tiny light-emitting diodes that are arranged around and optically isolated from a microscope tube. The green light is transmitted through nonkeratinized mucosa and absorbed by hemoglobin; thus, red blood cells (RBCs) appear as dark globules. The captured videos provide sharp contour visualization of the microcirculation and show flowing RBCs, plasma gaps, and leukocytes. The IDF handheld vital microscope captures images at a rate of 25 frames/s; 100 frames are recorded in each video clip.

Study Protocol

The probe was handheld during microcirculatory measurements. Various precautions were taken and steps followed in line with international guidelines [19–21] to obtain images of adequate quality and to ensure satisfactory reproducibility. First, focus and illumination were adjusted. At each time point, three steady images of 4 s were acquired and stored on a computer in accordance with the international guidelines on sublingual microcirculation [19–21]. The image clips were exported using the embedded CC-tools software (CytoCam, Braedius Medical). Images that were captured after the induction of anesthesia (T_0) and after CPB (10 min after protamine administration) (T_1) were used.

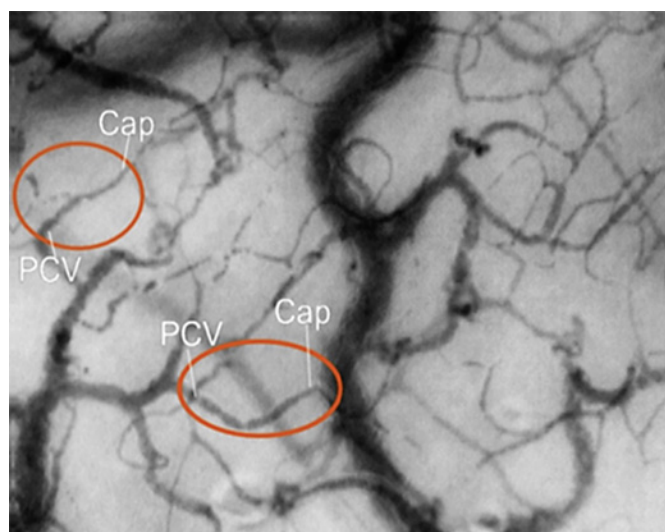
Image Acquisition

The complete data set of 60 videos was assessed according to the Microcirculation Image Quality Score [19] in line with international consensus [20, 21]. Sixteen videos were excluded from analysis due to unacceptable image quality. There was no loss of patients or time points, as these excluded videos were dispersed among patients and time points. The 44 sublingual video clips that showed at least one capillary-postcapillary venule (C-PCV) unit were included for further analysis. The selection criterion that was used to define a C-PCV vessel segment was as follows: a non-branched capillary merges into a postcapillary venule (PCV) (a small venule that is distal to the capillary) with no branching vessels present (Fig. 1). Study of the C-PCV unit enables tracking of white globules (leukocytes) from the capillary into the PCV along a single C-PCV segment. The use of the C-PCVs was described in detail previously [15]. The selected C-PCV units were excluded from the analysis if they were out of focus, if the video was unstable, or if no flow or intermittent flow that was induced by the iatrogenic pressure appeared. After application of these exclusion criteria, the video clips were analyzed via the method described below.

Image Analysis

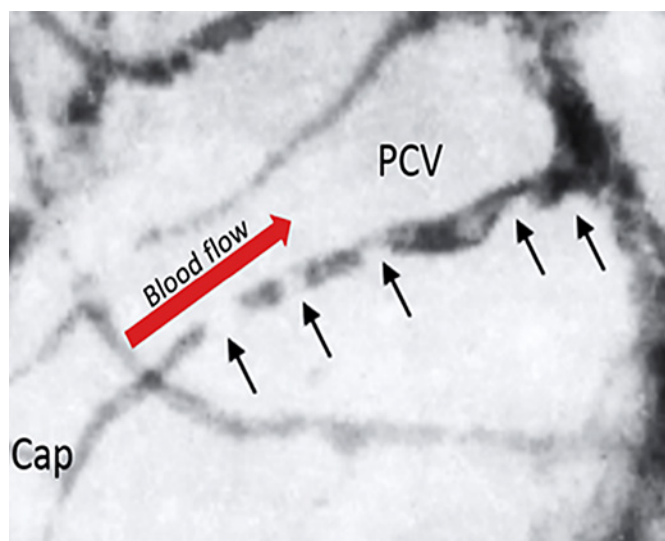
Video clips were analyzed using the method of frame averaging. The analysis was conducted blindly by an experienced observer, and the same video clips and the same C-PCVs were reviewed by a second observer to determine interrater agreement.

The method of frame averaging was developed as a technique for differentiating between plasma gaps and leukocytes [18]. In the conventional identification and manual counting process, leukocytes and plasma gaps appear as moving white globules that are surrounded by dark RBCs. While leukocytes maintain their shape, plasma gaps change continuously in terms of shape and volume [15]. Figure 2 shows leukocytes rolling along the endothelium, thereby maintaining their distinctive form.



Color version available online

Fig. 1. Screenshot of the sublingual microcirculation video clip that was obtained via CytoCam-IDF imaging. Each of the two red circles contains a C-PCV unit. The units in the image exhibit a nonbranched aspect and are observed as a single unit. The selection of the C-PCV unit is important for the study of leukocyte kinetics as it enables the tracking of white globules (leukocytes) from the Cap into the PCV, where leukocyte velocity changes due to sticking and rolling. Cap, capillary; C-PCV, capillary-postcapillary venule; IDF, incident dark-field; PCV, postcapillary venule.



Color version available online

Fig. 2. Rolling leukocytes in the sublingual microcirculation. A screenshot of a sublingual microcirculation image that was obtained via the CytoCam-IDF imaging is presented, which shows a superimposed image of a Cap that is merging into a PCV. The rolling leukocytes are identified by black arrows. Cap, capillary; IDF, incident dark-field; PCV, postcapillary venule.

Fig. 3. Method of frame averaging. The light gray boxes represent individual frames from the original video clips, which are also known as input frames and denoted by $I(n)$. The darker gray boxes represent the new frames that are created via averaging and the output frame is denoted by $J(n)$. $J(n)$ can be calculated via the following formula:

$$J(n) = \sum_{i=-\frac{k-1}{2}}^{\frac{k-1}{2}} \left[h(i) \times I(n+i) \right].$$

When $k = 3$, the weighted average of three consecutive frames was calculated, as shown in the figure. Similarly, when $k = 7$, the weighted average of seven consecutive frames was calculated. In each case, k must be an odd number. The weighted average was calculated using the Gaussian function $h(n)$.

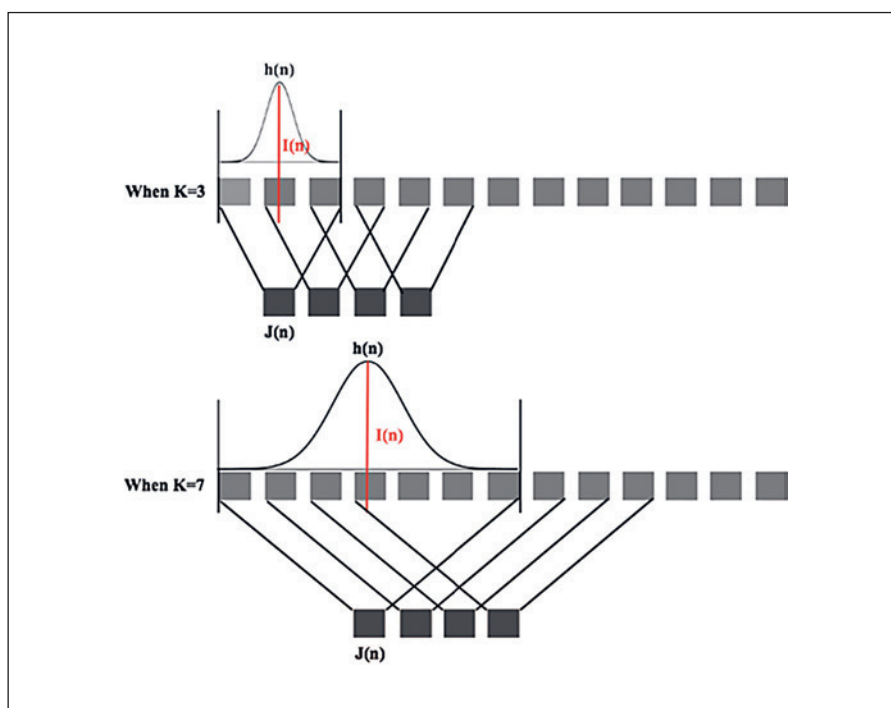


Table 1. Demographic data

| | |
|---------------------------------|------------|
| Age, years | 63.6±5.5 |
| Sex ratio (male:female) | 10:0 |
| Body mass index | 27.7±2.6 |
| Cardiac surgery with CPB, % | 100 |
| Duration of CPB, min | 85±21.3 |
| Duration of cross-clamping, min | 44.1±13.3 |
| Duration of surgery, min | 230.5±49.2 |
| Number of CABG patients | 10 |
| Number of grafts/patient | 3.6±1.0 |

Values are presented as mean ± standard deviation. CABG, coronary artery bypass grafting; CPB, cardiopulmonary bypass.

As discussed above, the IDF camera captures images with a frame rate of 25 frames/s and an extremely short exposure time of 2 ms/frame. In the method of frame averaging, each video frame is composed of a weighted average of neighboring video frames in time, which effectively simulates an increased exposure time at each frame (Fig. 3). Then, the frame-averaged videos are slowed to 7, 9, or 12 frames/s to produce a third generation of video clips using a software that was developed by the authors (MATLAB; Mathworks, Natick, MA, USA). Slowing the video frame rate increased the visibility of the slowly-moving leukocytes within the C-PCV units against blurred plasma gaps and RBCs. Finally, using the frame-averaged video clips, the rolling leukocytes were identified and counted based on their kinetics, and the number of leukocytes/C-PCV unit/4 s (L/C-PCV/4 s) was reported.

Table 2. Hemodynamic parameters, body temperature, and laboratory data

| Parameters | T ₀ | T ₁ |
|--------------------------------|----------------|----------------|
| Heart rate, bpm | 55±11.7 | 70.5±10.3** |
| Mean arterial pressure, mm Hg | 86.8±15.6 | 67.7±11.7* |
| Body temperature, °C | 36.0±0.3 | 36.7±0.3** |
| Hemoglobin concentration, g/dL | 12.7±0.8 | 9.6±0.9*** |
| Lactate, mmol/L | 1.2±0.5 | 1.5±0.3 |
| pH | 7.4±0.02 | 7.4±0.04 |
| HCO ₃ , mmol/L | 24.6±1.2 | 23.8±1.7 |

Values are presented as mean ± standard deviation. Data were tested with paired Student *t* test. T₀, after the induction of anesthesia; T₁, after cardiopulmonary bypass (10 min after protamine administration). **p* < 0.05, ***p* < 0.001, ****p* < 0.0001.

Statistical Analysis

Data were analyzed using GraphPad Prism 6.0 (GraphPad Software, San Diego, CA, USA) by an independent researcher. All values are expressed as the mean ± standard deviation or median with interquartile range. The Shapiro-Wilk normality test was used to determine whether the data were distributed normally. As the data of rolling microcirculatory leukocytes did not follow a normal distribution, a nonparametric test (the Wilcoxon matched-pair signed-rank test) was performed to analyze these data. After identifying a normal distribution, the paired *t* test was used to analyze the systemic leukocyte count, the percent change in leukocyte counts (rolling leukocytes vs. systemic leukocytes), and the ratio

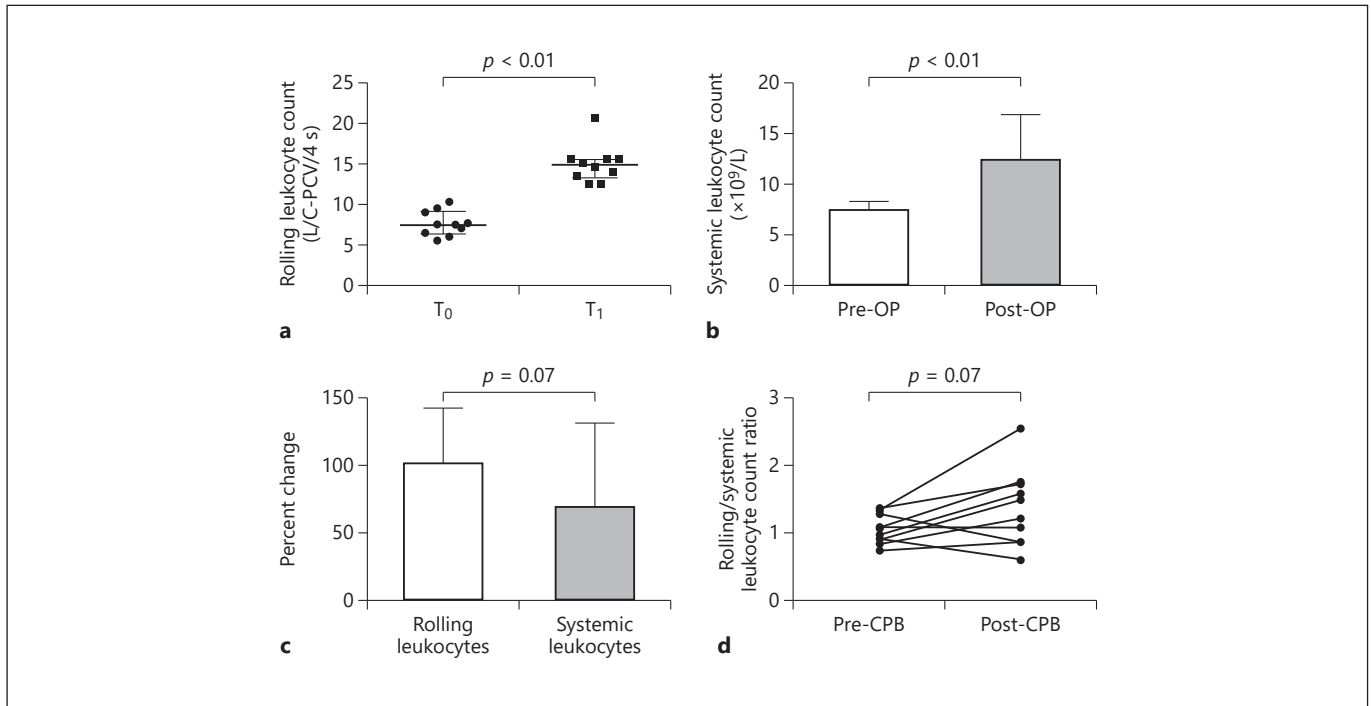


Fig. 4. Microcirculatory and systemic leukocyte values. **a** Median number (interquartile range) of rolling leukocytes within the sublingual microcirculation of 10 CABG patients at two time points. The median number (interquartile range) of rolling leukocytes is significantly increased from T₀ (7.5 [6.4–9.1] L/C-PCV/4 s) to T₁ (14.8 [13.2–15.5] L/C-PCV/4 s). **b** Systemic leukocyte count: number of systemic leukocytes was increased from $7.4 \pm 0.9 \times 10^9$ /L preoperatively (Pre-OP) to $12.4 \pm 4.4 \times 10^9$ /L postoperative (Post-OP). **c** Percent changes in leukocyte counts: the rolling microcirculatory leukocytes (from T₀ to T₁) versus the systemic leukocytes

(from the preoperative to the postoperative state). **d** Ratio of the rolling leukocyte count to the systemic leukocyte count. The ratio is shown as an individual line for each patient, with an overall increase from pre-CPB to post-CPB ($p = 0.07$). The data were evaluated with the Wilcoxon matched-pair signed-rank test and the paired *t* test for **a** and **b–d**, respectively. CABG, coronary artery bypass grafting; CPB, cardiopulmonary bypass; L/C-PCV/4 s, number of leukocytes/capillary-postcapillary venule unit/4 s; T₀, after the induction of anesthesia; T₁, after cardiopulmonary bypass (10 min after protamine administration).

between the microcirculatory rolling leukocyte count and the systemic white blood cell (WBC) count. A p value < 0.05 was considered statistically significant. The interrater agreement was determined via Bland-Altman analysis.

Results

Patient characteristics are presented in Table 1. Intraoperative hemodynamic parameters, body temperature, and arterial blood gas analysis are summarized in Table 2.

Figure 4a shows the numbers of rolling leukocytes in the sublingual microcirculation at T₀ and T₁ that were obtained from 10 on-pump CABG patients. According to image analysis, the number of rolling leukocytes increased from T₀ (7.5 [6.4–9.1] L/C-PCV/4 s) to T₁ (14.8 [13.2–15.5] L/C-PCV/4 s) ($p < 0.01$). The systemic leukocyte count is plotted in Figure 4b. A significant in-

crease in the systemic leukocyte count from $7.4 \pm 0.9 \times 10^9$ /L (preoperative) to $12.4 \pm 4.4 \times 10^9$ /L (postoperative) ($p < 0.01$) was also detected. Figure 4c shows the percent changes in the microcirculatory and systemic leukocyte counts. The percent change in the leukocyte count was found to be higher in the sublingual microcirculation than systemically ($p = 0.07$). Figure 4d plots the ratio between the number of rolling leukocytes and systemic WBCs of each patient. An increase in the ratio of the rolling leukocyte count to the systemic WBC count was observed from pre-CPB to post-CPB ($p = 0.07$).

Regarding the interrater variability of the method of frame averaging, according to Bland-Altman analysis, the interrater agreement between the observers was satisfactory, with a mean difference of 0.5643 L/C-PCV/4 s and limits of agreement that ranged from –3.665 to 4.793 L/C-PCV/4 s.

Discussion

In the current study, we visualized the leukocyte-endothelium interaction in the sublingual microcirculation of CABG patients by applying the method of frame averaging to IDF imaging for the first time. The application of this methodology to IDF imaging enabled the identification and quantification of rolling leukocytes by providing a technique for differentiating between plasma gaps and leukocytes.

Although HVM devices offer a noninvasive method for observing the microcirculation and are feasible for bedside measurements, limited data are available on leukocyte counting and identifying the leukocyte-endothelium interaction in the human microcirculation during cardiac surgery. Bauer et al. [14] were the first to identify rolling leukocytes using HVM and a conventional manual methodology in sublingual recordings in cardiac surgery patients. Via visual inspection, they identified the leukocytes as a void in the erythrocyte column that showed slow pattern of movement along the vessel wall. The authors quantitatively assessed the number of rolling leukocytes by subdividing the screen of a high-resolution monitor into nine rectangles. In 8 patients, they counted the numbers of PCVs and capillaries in each square and the number of rolling leukocytes that could be identified in each PCV, which was expressed in terms of rolling leukocytes/20 s. The authors demonstrated a higher increase in microcirculatory rolling leukocytes compared to the systemic leukocyte count, which is in accordance with the results of the current study. The main challenge in identifying leukocytes using HVM is distinguishing leukocytes from plasma gaps. This is because HVM uses green light to identify RBCs (green light is absorbed by hemoglobin), which appear as dark globules, but lacks optical contrast for leukocytes and plasma gaps, which appear as white structures against a white background. Applying the conventional methodology to OPS imaging, which has a lower resolution than the IDF technique that was used in the present study [6, 8], Bauer et al. [14] were unable to distinguish between leukocytes and plasma gaps in the venules. According to the authors, plasma gaps may be falsely identified as leukocytes or may contain leukocytes that are not detected since no erythrocytes are present to provide the necessary contrast. Moreover, microvascular hematocrit and blood flow, which changes during CPB, may affect the visualization of leukocytes.

Recently, our group proposed a space-time diagram analysis method to study leukocyte kinetics and functions

in the microcirculation [15]. The space-time diagram analysis method realized higher reproducibility than conventional counting. This methodology enabled the identification of rolling and nonrolling leukocytes in the sublingual microcirculation and the quantitative measurement of leukocyte velocity. However, a limitation of space-time diagram analysis in microvascular image analysis software (AVA) is the necessity of performing the labor-intensive manual steps (velocity estimations, manual vessel drawing, and detected vessel selection) in which the space-time diagrams are generated. Currently, only by using the original version of AVA (AVA 3.2), which is based on the paper of Dobbe et al. [16], is it possible to generate the space-time diagrams.

The method of frame averaging was developed as a technique for differentiating between plasma gaps and leukocytes [18]. This methodology was first applied to SDF imaging in sepsis patients [18]. Fabian-Jessing et al. [18] identified higher numbers of rolling and adhered leukocytes in patients with septic shock compared to noninfected controls and an increased number of adhered leukocytes in nonsurvivors. However, the authors failed to consider the systemic WBC count.

The significant increase in the number of rolling leukocytes detected in the current study supports the occurrence of a systemic inflammatory reaction during CPB. This is corroborated by the increased systemic leukocyte counts in these patients which were measured before and after the operation. Additionally, the percent change in leukocyte count was found to be higher in the sublingual microcirculation, while the ratio between the microcirculatory activated leukocytes and systemic WBC count increased from pre-CPB to post-CPB. This ratio was used by the authors to evaluate whether the increased number of microcirculatory activated leukocytes is caused by endothelial activation due to systemic inflammatory response that is independent of the increase in the overall number of circulating WBCs.

Degradation of the endothelial glycocalyx precedes the expression of endothelial adhesion molecules that are attached to the endothelial surface, which enables sticking and rolling of leukocytes and, in turn, precedes paracellular and transcellular diapedesis [22]. Thus, the detection of rolling leukocytes on the endothelial surface is an indirect demonstration of a compromised glycocalyx as part of the innate immune response and, hence, constitutes an important clinical observation of the presence of a (micro)vascular pathology [23].

Few bedside methodologies other than the use of biomarkers can detect these events at the cellular level. The

IDF device consists of a computer-controlled, high-resolution image sensor which, in combination with a specially designed microscope lens, produces high-resolution images in which 30% more sublingual capillaries can be detected compared to the previous-generation devices [6]. The ability to directly visualize the kinetics of the leukocyte-endothelium interaction using IDF imaging, particularly in cardiac surgery patients, may facilitate the diagnosis of systemic inflammatory response after CPB by identifying rolling leukocytes along the microcirculatory endothelium, and may provide important clinical feedback regarding treatment efficacy by demonstrating its resolution following treatment strategies and facilitating the determination of an optimal therapeutic dose.

A limitation of the current study concerns the small number of patients in a single center. Nevertheless, our study demonstrates that the number of rolling leukocytes was significantly increased after discontinuation of CPB. However, nonrolling leukocytes could not be counted. This is a shortcoming of the frame averaging method in contrast to the space-time diagram methodology [15], which enables the counting of rolling and nonrolling leukocytes and the determination of their velocities. In addition, no additional inflammatory biomarkers and no microcirculatory parameters were studied to validate our measurements. Moreover, the observed drop in hemoglobin concentration could have affected the image contrast between RBCs and leukocytes. We expect that this methodology can be refined to overcome these shortcomings.

Conclusion

The ability to directly visualize the kinetics of the leukocyte-endothelium interaction using IDF imaging facilitates the diagnosis of systemic inflammatory response syndrome after CPB via identification of rolling leukocytes. Integration of the frame averaging algorithm into the future software developments of handheld vital microscopes may enable the use of microcirculatory leukocyte count as real-time clinical parameter at the bedside.

Acknowledgments

The authors would like to thank all subjects who participated in this research. They would also like to thank the operating room personnel for their participation and assistance during the measurements.

Statements of Ethics

Ethics approval was granted by the Ethics Committee of Acibadem Mehmet Ali Aydınlar University School of Medicine (ATADEK 2013-540). All procedures in the study were in accordance with the Declaration of Helsinki. Written informed consent was obtained from all participants.

Disclosure Statement

Dr. C. Ince has developed SDF imaging and is listed as an inventor on related patents that were commercialized by MicroVision Medical under a license from the Academic Medical Center. He receives no royalties or benefits from this license. He has been a consultant for MicroVision Medical in the past, but has not been involved with this company for more than 5 years and holds no shares or stock. Braedius Medical, which is a company owned by a relative of Dr. C. Ince, has developed and designed a handheld microscope (the CytoCam-IDF imaging microscope). Dr. C. Ince has no financial relationship with Braedius Medical of any sort (he has never owned shares or received consultancy or speaker fees from Braedius Medical). Dr. C. Ince runs an internet site (www.microcirculationacademy.org) that offers services (e.g., training, courses, and analysis) that are related to clinical microcirculation. The other authors declare that they have no competing interests.

Funding Sources

This research received no funding.

Author Contributions

Z. Uz and G. Aykut participated in the design of the study, performed the IDF imaging, performed the analysis, participated in the interpretation and writing of the manuscript, and drafted and revised the manuscript. M. Massey developed the frame averaging technique and the software that was used for preprocessing. C. Ince participated in the design of the study, contributed to manuscript revision, and is the guarantor of the study. T.M. van Gulik and F. Toraman contributed to manuscript revision and interpretation. Y. Ince and L. Shen contributed to image development and manuscript revision. B. Ergin performed the statistical analyses. All authors read and approved the final manuscript.

References

- 1 Bronicki RA, Hall M. Cardiopulmonary bypass-induced inflammatory response: pathophysiology and treatment. *Pediatr Crit Care Med*. 2016 Aug;17(8 Suppl 1):S272–8.
- 2 Laffey JG, Boylan JF, Cheng DC. The systemic inflammatory response to cardiac surgery: implications for the anesthesiologist. *Anesthesiology*. 2002 Jul;97(1):215–52.

- 3 Xing K, Murthy S, Liles WC, Singh JM. Clinical utility of biomarkers of endothelial activation in sepsis – a systematic review. *Crit Care*. 2012 Jan;16(1):R7.
- 4 Boyle EM Jr, Morgan EN, Kovacich JC, Canty TG Jr, Verrier ED. Microvascular responses to cardiopulmonary bypass. *J Cardiothorac Vasc Anesth*. 1999 Aug;13(4 Suppl 1):30–5; discussion 36–7.
- 5 Hernandez G, Bruhn A, Ince C. Microcirculation in sepsis: new perspectives. *Curr Vasc Pharmacol*. 2013 Mar;11(2):161–9.
- 6 Aykut G, Veenstra G, Scorcella C, Ince C, Boerma C. Cytocam-IDF (incident dark field illumination) imaging for bedside monitoring of the microcirculation. *Intensive Care Med Exp*. 2015 Dec;3(1):40.
- 7 Goedhart PT, Khalilzade M, Bezemer R, Merza J, Ince C. Sidestream Dark Field (SDF) imaging: a novel stroboscopic LED ring-based imaging modality for clinical assessment of the microcirculation. *Opt Express*. 2007 Nov;15(23):15101–14.
- 8 Groner W, Winkelman JW, Harris AG, Ince C, Bouma GJ, Messmer K, et al. Orthogonal polarization spectral imaging: a new method for study of the microcirculation. *Nat Med*. 1999 Oct;5(10):1209–12.
- 9 De Backer D, Donadello K, Sakr Y, Ospina-Tascon G, Salgado D, Scolletta S, et al. Microcirculatory alterations in patients with severe sepsis: impact of time of assessment and relationship with outcome. *Crit Care Med*. 2013 Mar;41(3):791–9.
- 10 Lundy DJ, Trzeciak S. Microcirculatory dysfunction in sepsis. *Crit Care Nurs Clin North Am*. 2011 Mar;23(1):67–77.
- 11 Nencioni A, Trzeciak S, Shapiro NI. The microcirculation as a diagnostic and therapeutic target in sepsis. *Intern Emerg Med*. 2009 Oct;4(5):413–8.
- 12 Omar YG, Massey M, Andersen LW, Giberson TA, Berg K, Cocchi MN, et al. Sublingual microcirculation is impaired in post-cardiac arrest patients. *Resuscitation*. 2013 Dec;84(12):1717–22.
- 13 Dekker NA, Veerhoek D, Koning NJ, van Leeuwen AL, Elbers PW, van den Brom CE, et al. Postoperative microcirculatory perfusion and endothelial glycocalyx shedding following cardiac surgery with cardiopulmonary bypass. *Anaesthesia*. 2019 May;74(5):609–18.
- 14 Bauer A, Kofler S, Thiel M, Eifert S, Christ F. Monitoring of the sublingual microcirculation in cardiac surgery using orthogonal polarization spectral imaging: preliminary results. *Anesthesiology*. 2007 Dec;107(6):939–45.
- 15 Uz Z, van Gulik TM, Aydemirli MD, Guerci P, Ince Y, Cuppen D, et al. Identification and quantification of human microcirculatory leukocytes using handheld video microscopes at the bedside. *J Appl Physiol (1985)*. 2018 Jun;124(6):1550–7.
- 16 Dobbe JG, Streekstra GJ, Atasever B, van Zijderveld R, Ince C. Measurement of functional microcirculatory geometry and velocity distributions using automated image analysis. *Med Biol Eng Comput*. 2008 Jul;46(7):659–70.
- 17 Boerma EC, Scheeren TW. Digging into the microcirculation: the rush for gold may excavate apples and oranges. *J Clin Monit Comput*. 2017 Aug;31(4):665–7.
- 18 Fabian-Jessing BK, Massey MJ, Filbin MR, Hou PC, Wang HE, Kirkegaard H, et al.; ProCESS Investigators. In vivo quantification of rolling and adhered leukocytes in human sepsis. *Crit Care*. 2018 Sep;22(1):240.
- 19 Massey MJ, Larochelle E, Najarro G, Karmacharla A, Arnold R, Trzeciak S, et al. The microcirculation image quality score: development and preliminary evaluation of a proposed approach to grading quality of image acquisition for bedside videomicroscopy. *J Crit Care*. 2013 Dec;28(6):913–7.
- 20 De Backer D, Hollenberg S, Boerma C, Goedhart P, Büchele G, Ospina-Tascon G, et al. How to evaluate the microcirculation: report of a round table conference. *Crit Care*. 2007;11(5):R101.
- 21 Ince C, Boerma EC, Cecconi M, De Backer D, Shapiro NI, Duranteau J, et al.; Cardiovascular Dynamics Section of the ESICM. Second consensus on the assessment of sublingual microcirculation in critically ill patients: results from a task force of the European Society of Intensive Care Medicine. *Intensive Care Med*. 2018 Mar;44(3):281–99.
- 22 Ince C, Mayeux PR, Nguyen T, Gomez H, Kellum JA, Ospina-Tascón GA, et al.; ADQI XIV Workgroup. ADQI XIV Workgroup. The endothelium in sepsis. *Shock*. 2016 Mar;45(3):259–70.
- 23 Donati A, Damiani E, Domizi R, Romano R, Adrario E, Peliaia P, et al. Alteration of the sublingual microvascular glycocalyx in critically ill patients. *Microvasc Res*. 2013 Nov;90:86–9.